

Integration of a Nanoporous Platinum Thin Film into a Microfluidic System for Non-enzymatic Electrochemical Glucose Sensing

Segyeong JOO,* Sejin PARK,** Taek Dong CHUNG,**† and Hee Chan KIM***†

**Interdisciplinary Program-Biomedical Engineering Major, Seoul National University, 28 Yongon-dong, Chongno-gu, Seoul 110-744, Korea*

***Center for Nano-Bio Applied Technology and Department of Chemistry, Sungshin Women's University, Seoul 136-742, Korea*

****Department of Biomedical Engineering, College of Medicine and Institute of Medical and Biological Engineering, Medical Research Center, Seoul National University, Seoul 110-744, Korea*

In this paper, we describe an amperometric-type enzymeless glucose sensing system based on a nanoporous platinum (Pt) electrode embedded in a microfluidic chip. This microchip system is comprised of a microfluidic transport channel network and a miniaturized electrochemical cell for nonenzymatic glucose sensing. Sample and buffer solutions were transferred to the cell by programmed electroosmotic flow (EOF). A nanoporous Pt electrode with the roughness factor of 200.6 was utilized to determine glucose concentrations in phosphate buffered saline (PBS) by the direct oxidation of glucose, without any separation process. The sensitivity of the developed system is $1.65 \mu\text{A cm}^{-2} \text{mM}^{-1}$ in the glucose concentration range from 1 - 10 mM in PBS.

(Received October 2, 2006; Accepted November 6, 2006; Published March 10, 2007)

Introduction

The most valuable advantage of the microfluidic systems for analytical purposes is their applicability to the rapid and accurate analysis of small sample volumes. This advantage has led to their being used in many electrophoretic separation applications,^{1,2} DNA analysis,³⁻⁵ cell manipulation,^{6,7} and immunoassays.⁸ In particular, recent advances in microfluidic control units such as pumps,^{9,10} valves,^{11,12} and mixers^{13,14} have resulted in the developments of microfluidic systems with complex fluidic channel networks that can perform highly sophisticated functions. Even though many of these microfluidic components have been demonstrated to work, the development of simpler, more reproducible, practical systems remains a key challenge.

In this respect, combinations of microfluidics with conventional chemical or biosensors potentially provide invaluable benefits for practical applications, because these systems do not require any additional unit for pretreatment, in particular, no separation step is needed. Conventional chemical or biosensors integrated in microfluidic systems function not only as detectors but also as separators, and thus they offer cost savings with respect to the complex peripherals required for sample pretreatments. On the other hand, microfluidic systems can perform functions that cannot be performed by chemical sensors or biosensors alone. For example, users can carry out accurate and convenient analyses due to the incorporation of an

automatic calibration module, which is operated by a microfluidic control program. By taking advantages of the inherent advantages of microfluidic chips, one can miniaturize the whole system and conduct entire analytical analyses on small samples. Moreover, the sophisticated integration of individual sensory system arrays in microfluidic networks allows simultaneous multiple analyses.¹⁵ In particular, electrochemical sensors may be incorporated into microfluidic systems to provide low cost, portable, and high-throughput analytical systems.

The reliable and cost-effective measurement of glucose in blood is obviously the most important biomedical analysis issue.^{16,17} Biological components, usually immobilized enzymes, in conventional glucose sensors cause intrinsic problems during manufacturing, storage, and distribution due to serious unacceptable dependences on temperature and humidity. Moreover, quality control difficulty and a short lifetime ultimately mean sizable costs. Furthermore, the integration of an enzyme-based glucose sensor and microfluidic systems restrict essential conventional chip fabrication processes, such as cleaning with acid/base/organic solutions or heat treatments, which is one reason why the development of an enzyme free glucose sensor is being pursued so energetically.

A number of reports have addressed the issue of nonenzymatic glucose sensing,¹⁸ and of these several methodologies, recent emphasis has been placed on the uses of nanoporous platinum (Pt) due to its simple fabrication, availability in micropattern form, and unique electrochemical features.¹⁹ Nanoporous platinum thin films are excellent glucose detectors, and substantially overcome the critical shortcomings of other enzymeless sensors.²⁰ Moreover, glucose

† To whom correspondence should be addressed.
E-mail: chembud@sungshin.ac.kr; hckim@snu.ac.kr

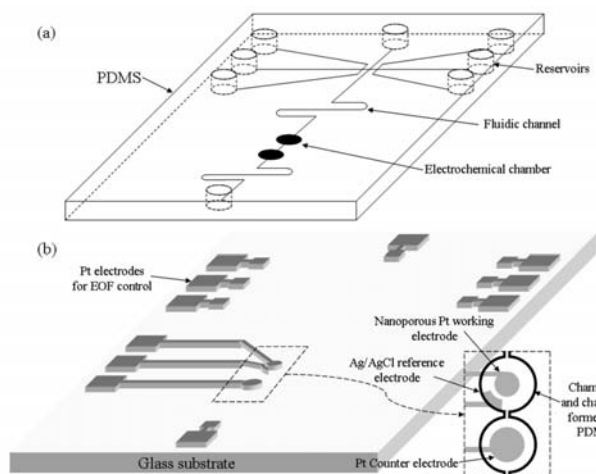


Fig. 1 Schematic diagram of the proposed microfluidic system. (a) The PDMS cover layer for channel, cells and reservoirs, and (b) the glass substrate for the Pt electrode patterns.

sensors based on nanoporous Pt technology are compatible with conventional microfabrication post-processing, since the electrode is composed of Pt. In addition, unlike pulsed amperometric detection,^{21,22} nanoporous Pt does not require a sample separation step, because its selectivity prevents REDOX interference by species like ascorbic acid or acetaminophen. Therefore, it is conceivable that a combination of nanoporous Pt with an appropriate microfluidic system handling sample solutions in a programmed sequence act as a nonenzymatic glucose sensor with useful additional functions, such as, automatic calibration, high-throughput analytical power, and reusability.

In order to demonstrate the feasibility of this concept, we integrated three electrodes into an electrochemical system on a microfluidic chip, *i.e.*, nanoporous Pt films as working and counter electrode and a silver/silver chloride (Ag/AgCl) solid state reference electrode. In this system, microfluidic sample delivery was driven by electroosmotic flow (EOF) control. In addition to investigating the operation of the integrated system, we also investigated its performance as a glucose sensor.

Experimental

System design

Figure 1 shows the schematic diagram of the proposed microfluidic system. Figure 1(a) describes the upper layer formed by poly(dimethyl siloxane) (PDMS), which contains the microfluidic channel network and reservoirs. Pt electrodes for EOF control and electrochemical detection were fashioned on the glass substrate, as shown in Fig. 1(b). The PDMS cover has 8 reservoirs of diameter 4 mm; 4 for samples, 1 for buffer, and 3 for waste. The microchannels connecting the reservoirs are 100 μm wide and 30 μm deep. The Pt electrodes for EOF control and electrochemical reactions were deposited on the bottoms of the 8 reservoirs and the electrochemical reaction cells, respectively. Two cells for electrochemical detection (one as a working and reference electrode and the other for counter electrode) have dimensions of 2 mm by 30 μm (diameter by height). Counter electrodes are segregated from working and reference electrodes to prevent working electrode contamination by products generated at the counter electrode during

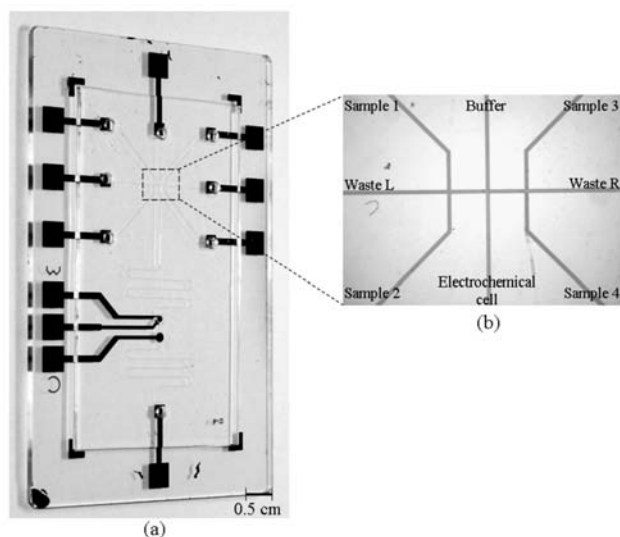


Fig. 2 (a) Photograph of the fabricated microfluidic system containing nanoporous Pt glucose sensor. (b) Enlarged view of the dashed area of (a), showing channel network connecting reservoirs.

electrochemical detection. The working electrode (diameter of 1 mm) is a nanoporous Pt film on a flat Pt pattern and the counter electrode (diameter of 1.5 mm) is a bare flat Pt pattern. The reference electrode used is an Ag/AgCl film on the bare Pt pattern.

Fabrication of the PDMS cover

A mold for the PDMS cast was made using epoxy-based negative photoresist (PR), named SU-8 (formulation 25, Microchem, Newton, MA). A 2" \times 3" pieces of soda-lime glass (Model S, Matsunami, Japan) was used as a substrate. After cleaning in a piranha solution ($\text{H}_2\text{SO}_4:\text{H}_2\text{O}_2 = 3:1$) for 10 min at 150°C, the slide glass was dehydrated on a hot plate for 3 min at 120°C. The adhesion between the cleaned glass substrate and PR was improved as follows: hexamethyldisilazane (HMDS) (J. T. Baker, USA) was spun-coated (SC-102, Won Corporation, Korea) for 30 s at 4000 rpm on the glass substrate, and then baked on a hot plate for 3 min at 120°C. The SU-8 spin-coating process was carried out for 30 s at 1500 rpm to obtain a 30 μm thick PR film. After two-step soft baking of the PR on a hot plate for 3 min at 65°C and 7 min at 95°C, the material was exposed to ultraviolet light (UV, 365 nm) at 300 mJ cm^{-2} under an appropriate photo mask using a mask aligner (MDA-400M, MIDAS System, Korea). For selective cross-linking of the exposed PR, a post exposure bake was performed on a hot plate for 1 min at 65°C and 3 min at 95°C. The exposed PR was developed using a developer solution (Developer for SU-8, Microchem) and then the patterned substrate mold was hardened by baking on a hot plate at 150°C for 10 min to increase its mechanical strength.

To prepare the cover PDMS layer containing channel patterns, we added 1 part of the curing agent (Sylgard 184 B, Dow Corning, Midland, MI) to the 10 parts of PDMS polymer base (Sylgard 184 A, Dow Corning). Mixing them thoroughly produced air bubbles, which were removed in a vacuum desiccator over 30 min. Finally, the mixture was poured onto the prepared SU-8 mold and cured thermally for 2 h at 60°C.

Metal patterns and electrode fabrication

A 2" \times 3" piece of soda-lime glass (Model S, Matsunami) was

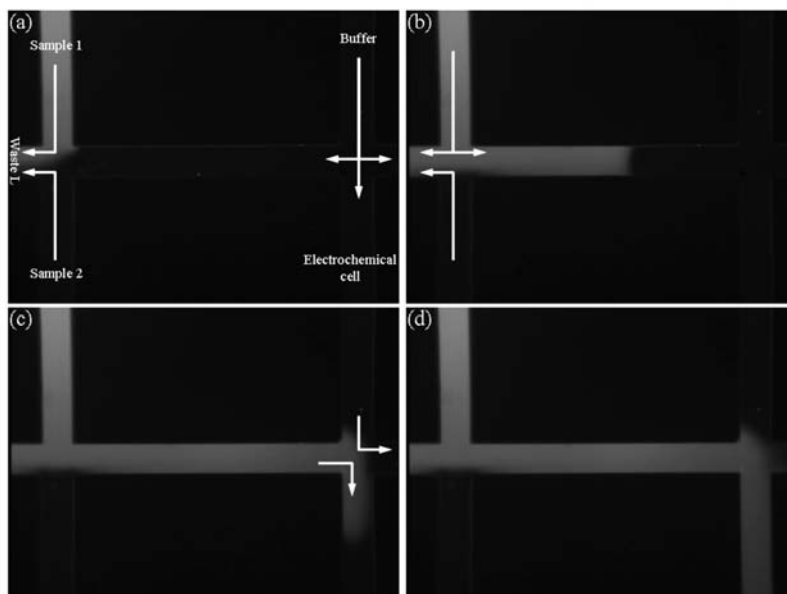


Fig. 3 The images showing the sequence from buffer loading condition to sample loading condition at (a) 0, (b) 6, (c) 13, (d) 20 s. White arrows indicate flow direction.

used as substrate for the metal patterns. After cleaning and HMDS coating, as described above, PR (AZ5214E, Clariant, Switzerland) was spun-coated for 30 s at 4000 rpm to obtain a 1.4 μm thick PR film. Soft baking of the PR on a hot plate for 1 min at 100°C and exposing it to 365 nm UV at 100 mJ cm^{-2} under an appropriate photo mask were then performed. For AZ5214E image reversal, another bake was performed on a hot plate for 5 min at 100°C and flood exposure was conducted at 400 mJ cm^{-2} at 365 nm without a mask. The PR was developed using an appropriate developer solution (AZ300MIF, Clariant).

A lift-off method was applied to obtain a patterned Ti/Pt film. A 100 nm thick Pt layer was deposited using a DC/RF magnetron sputter (Atek, Korea) on a the 20 nm thick titanium (Ti) layer (an adhesion promoter on patterned PR). The glass substrate was then immersed into acetone to remove the Pt film and the PR layer underneath.

Nanoporous Pt films were electrochemically deposited on the working electrode using liquid crystal as described in a previous paper.²⁰ Silver (Ag) was electroplated on the Pt film of reference electrode areas using a commercial Ag electroplating agent (Hanyang Chemical, Korea). One micrometer thick Ag film was formed by applying a constant potential ($-1.0 \text{ V vs. Ag/AgCl}$) using a potentiostat (CHI750A, CH Instrument, Austin, TX). A portion of the electroplated Ag film was oxidized by applying a constant potential (0.4 V vs. Ag/AgCl) in a 3 M KCl solution, to produce a solid state Ag/AgCl reference electrode on the microfluidic chip.

The PDMS cover and the glass substrate with metal patterns were then plasma-treated in an air plasma cleaner/sterilizer (RGD-100, Reflex Analytical, Ridgewood, NJ) for 1 min. Satisfactory bonding and alignment were achieved.

Results and Discussion

Figure 2 shows the fabricated microfluidic system in which a nanoporous Pt electrochemical glucose detector was embedded. Figure 2(b) is an enlarged view of the dashed area in Fig. 2(a),

which schematically illustrates the channel network connecting 8 reservoirs named samples 1 – 4, buffer, waste R, waste L, and waste.

Sample delivery using EOF control

Fluids on the microfluidic chip were controlled using 8 electrodes on 8 reservoirs. Fluorescent dye (Rhodamine B (10 mM), Aldrich, Milwaukee, WI) diluted in 0.1 M phosphate buffered saline (PBS) at pH 7.4 was filled into the sample 1 reservoir and all other reservoirs were filled with PBS. Using this configuration, buffer solution and sample flows could be switched between toward the waste and toward the electrochemical cell by the controlling the applied potential program. Figure 3 shows step-by-step changes of flow directions for loading the fluorescent dye solution (sample 1) into the electrochemical cell. Figure 3(a) shows the buffer loading step, during which the buffer solution flows to the electrochemical cell and the sample solution from the sample 1 reservoir moves to the Waste L. On changing the potentials applied to the reservoirs, the sample solution in the sample 1 reservoir moves to the electrochemical cell while the buffer solution moves to Waste R (Fig. 3(d)). Figure 3(b) shows that the flow characteristics are not parabolic but flat in shape, which is a characteristic of EOF. Solutions in samples 2 – 4 could be delivered to the electrochemical cell in the same manner. The potentials applied to the 8 electrodes in the 8 reservoirs for loading buffer and sample are summarized in Table 1.

Nanoporous Pt electrode test

The effective surface area of the fabricated nanoporous Pt electrode on the chip was characterized by measuring the roughness factor. Figure 4 shows the cyclic voltammogram of the fabricated nanoporous Pt electrode in 1 M sulfuric acid. Reportedly, electrochemical reduction of the hydrogen fully adsorbed on Pt surface produces 210 $\mu\text{C cm}^{-2}$.²³ Thus, the area under the hydrogen adsorption/desorption peak reveals information about the roughness factor. From the measured charge of 330.7 μC in Fig. 4, the surface area of the flat Pt was

Table 1 Programs for five different EOF control conditions (applied potential/kV)

Condition	Buffer	Sample 1	Waste L	Sample 2	Waste	Sample 3	Waster R	Sample 4
Buffer loading	1.0	0.95	0.90	0.95	0	0.95	0.90	0.95
Sample 1 loading	0.95	1.0	0.90	0.95	0	0.95	0.90	0.95
Sample 2 loading	0.95	0.95	0.90	1.0	0	0.95	0.90	0.95
Sample 3 loading	0.95	0.95	0.90	0.95	0	1.0	0.90	0.95
Sample 4 loading	0.95	0.95	0.90	0.95	0	0.95	0.90	1.0

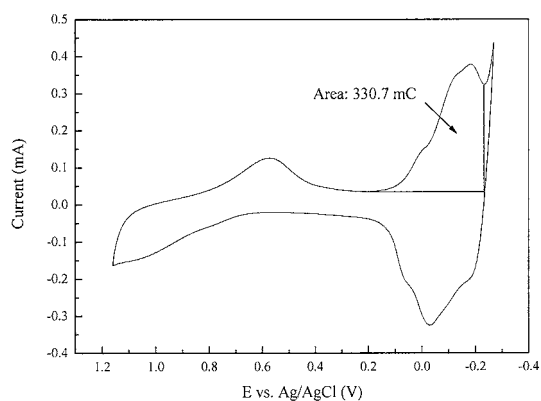


Fig. 4 Cyclic voltammogram of the fabricated nanoporous Pt electrode in 1 M sulfuric acid.

calculated to be $7.85 \times 10^{-3} \text{ cm}^2$, which corresponds to a roughness factor of 200.6. This indicates that the surface area of the described nanoporous Pt electrodes is 200.6 times larger than that of a flat Pt electrode with the same projected surface area.

Glucose sensor test

The performance of the developed microfluidic system as a glucose sensor was evaluated at a number of glucose concentrations. Figure 5(a) shows the chronoamperometric responses to 0, 1, 3, 5, 10, 15, and 20 mM glucose solutions diluted in PBS at an applied voltage of 0.4 V versus the solid-state Ag/AgCl reference electrode. The calibration curve in Fig. 5(b) was obtained by measuring current values over 15 s at each glucose concentration. Responses were linearly dependent on glucose concentration in the range 1 to 10 mM with the sensitivity of $1.65 \mu\text{A cm}^{-2} \text{ mM}^{-1}$. In addition, the calculated limit of the unit was 0.097 mM, which is the concentration corresponding to signal to noise ratio (S/N) of 4.

Conclusion

Here, we describe a microfluidic system containing an embedded novel non-enzymatic glucose detector. A nanoporous Pt electrode and a solid-state Ag/AgCl reference electrode were compactly integrated on a microfluidic chip to produce an electrochemical detector. The solutions from four sample reservoirs were delivered to the electrochemical cell under individual control using an appropriate potential program, the operabilities of which was verified using fluorescent dye experiments. The nanoporous Pt electrode fabricated on the chip was characterized electrochemically by measuring the hydrogen adsorption/desorption peak area in the cyclic voltammogram, which indicated that the devised electrodes had

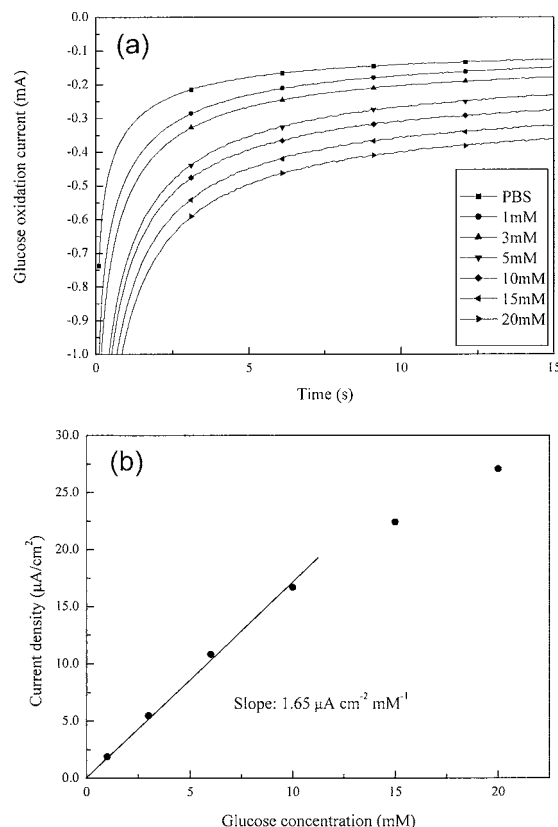


Fig. 5 (a) Chronoamperometric data of glucose oxidation current for 1, 3, 6, 10, 15 and 20 mM glucose solution in PBS buffer. (b) The corresponding calibration curve.

a roughness factor of 200.6. Amperometric analysis of aqueous glucose in PBS was conducted at a series of glucose concentrations using the developed system. The calibration curve showed that the devised system responds linearly to glucose across the 1–10 mM concentration range with the sensitivity of $1.65 \mu\text{A cm}^{-2} \text{ mM}^{-1}$ and a test time of 15 s. The calculated detection limit of the developed system was 0.097 mM.

The paper describes the first example of a microfluidic system containing a nanoporous Pt electrode for nonenzymatic glucose analysis. Programmed fluidic control of multiple reservoirs suggests possibilities of high-throughput analysis, automatic calibration, and multiple use. To realize the proposed goals, subsequent studies are in progress, including the replacement of the Ag/AgCl reference electrode with a more stable solid-state reference electrode, automatic calibration and refreshment process, and the development of a pretreatment unit for practical analysis, including blood glucose level determination. In addition, in order to extend the use of the developed system to

actual biological samples, such as serum or blood, it is necessary to develop an appropriate layer, which would protect the electrode from contamination by protein or other material without reducing sensitivity and selectivity seriously. We have made considerable progress in this issue, as will be reported in a separate paper.

Acknowledgements

This work was supported by the Korea Science and Engineering Foundation through the Advanced Biometric Research Center (HCK) and by the grant No. R01-2006-000-10240-0 from the Basic Research Program of the Korea Science & Engineering Foundation (TDC).

References

1. C. S. Effenhauser, A. Manz, and H. M. Widmer, *Anal. Chem.*, **1995**, *67*, 2284.
 2. F. V. Heeren, E. Verpoorte, A. Manz, and W. Thormann, *J. Microcolumn Sep.*, **1996**, *8*, 373.
 3. S. C. Jacobson and J. M. Ramsey, *Anal. Chem.*, **1996**, *68*, 720.
 4. J. H. Daniel, S. Iqbal, R. B. Millington, D. F. Moore, C. R. Lowe, D. L. Leslie, M. A. Lee, and M. J. Pearce, *Sens. Actuators, A*, **1998**, *71*, 81.
 5. K. Hosokawa, K. Sato, N. Ichikawa, and M. Maeda, *Lab Chip*, **2004**, *4*, 181.
 6. P. C. H. Li and D. J. Harrison, *Anal. Chem.*, **1997**, *69*, 1564.
 7. F. Arai, C. Ng, H. Maruyama, A. Ichikawa, H. El-Shimy, and T. Fukuda, *Lab Chip*, **2005**, *5*, 1399.
 8. L. B. Koutny, D. Schmalzing, T. A. Taylor, and M. Fuchs, *Anal. Chem.*, **1996**, *68*, 18.
 9. M. Koch, A. G. R. Evans, and A. Brunnschweiler, *J. Micromech. Microeng.*, **1998**, *8*, 119.
 10. A. V. Lemoff and A. P. Lee, *Sens. Actuators, B*, **2000**, *63*, 178.
 11. X. Yang, C. Grosjean, and Y.-C. Tai, *J. Microelectromech. Syst.*, **1999**, *8*, 393.
 12. P. K. Yuen, L. J. Kricka, and P. Wilding, *J. Micromech. Microeng.*, **2000**, *10*, 401.
 13. D. Catelain, M. Koch, A. G. R. Evans, and A. Brunnschweiler, *J. Micromech. Microeng.*, **1998**, *8*, 123.
 14. F. G. Bessoth, A. J. deMello, and A. Manz, *Anal. Commun.*, **1999**, *36*, 213.
 15. R.-H. Horng, P. Han, H.-Y. Chen, K.-W. Lin, T.-M. Tsai, and J.-M. Zen, *J. Micromech. Microeng.*, **2005**, *15*, 6.
 16. F. Scheller and F. Schubert, "Biosensors", **1992**, Elsevier, Amsterdam.
 17. G. S. Wilson, "Bioelectrochemistry", **2002**, Vol. 9, Wiley-VCH, Weinheim.
 18. S. Park, H. Boo, and T. D. Chung, *Anal. Chim. Acta*, **2006**, *556*, 46.
 19. H. Boo, S. Park, B. Ku, Y. Kim, J. H. Park, H. C. Kim, and T. D. Chung, *J. Am. Chem. Soc.*, **2004**, *126*, 4524.
 20. S. Park, T. D. Chung, and H. C. Kim, *Anal. Chem.*, **2003**, *75*, 3046.
 21. D. S. Bindra and G. S. Wilson, *Anal. Chem.*, **1989**, *61*, 2566.
 22. C. D. Garcia and C. S. Henry, *Anal. Chem.*, **2003**, *75*, 4778.
 23. S. Trasatti and O. A. Petrii, *J. Electroanal. Chem.*, **1992**, *327*, 353.
-